ELSEVIER

Journal of Alloys and Compounds 300–301 (2000) 218–223

Journal of ALLOYS AND COMPOUNDS

www.elsevier.com/locate/jallcom

Excited state absorption processes in Sm^{3+} doped GdOCl☆

Sami Areva[a,b], Jorma Hölsä[a,*], Ralf-Johan Lamminmäki[a,b], Hanna Rahiala[b,c], Przemysław Dereń[d], Wiesław Stręk[d]

[a]*University of Turku, Department of Chemistry, FIN-20014 Turku, Finland*
[b]*Graduate School of Materials Research, Turku, Finland*
[c]*Åbo Akademi University, Department of Physical Chemistry, FIN-20500 Turku, Finland*
[d]*Polish Academy of Sciences, Institute of Low Temperature and Structure Research, P.O. Box 937, PL-50 950 Wroclaw, Poland*

Abstract

The FT-Raman spectrum of the polycrystalline GdOCl doped with 1 mol% Sm^{3+} was measured at room temperature using a cw Nd:YAG laser with the excitation wavelength of 1064 nm (9400 cm^{-1}). Besides the very weak Stokes and anti-Stokes Raman lines the additional strong lines were concluded to result from luminescence processes. The UV–Vis–NIR absorption spectra of GdOCl:Sm^{3+} (x_{Sm}=0.06) and the energy level simulation of Sm^{3+} in SmOCl yielded the energy level scheme of Sm^{3+}. The additional lines could be assigned to the IR and visible Stokes and anti-Stokes luminescence of Sm^{3+}. Absorption of the 9400 cm^{-1} photons leads first to transition to the $^6F_{9/2}$ and then to the $^4F_{3/2}$ energy level of Sm^{3+}. The lines corresponding to luminescence at 13 596 and 12 310 cm^{-1} could then be assigned to the anti-Stokes transitions from the $^4F_{3/2}$ energy level to the $^6H_{13/2}$ and $^6H_{15/2}$ levels, respectively. Also lines in the Stokes emission originate from the luminescence processes of Sm^{3+}. However, all the extra lines in the Raman spectrum have not yet been explained by the luminescence processes.

Keywords: Excited state absorption; Anti-Stokes luminescence; Samarium oxychloride

1. Introduction

Up-conversion from IR radiation to visible light or UV radiation has been reported for several rare earths (RE), e.g. Pr^{3+}, Eu^{3+}, Er^{3+}, Ho^{3+} and Tm^{3+} [1–10]. These studies have been focused to develop solid state up-conversion lasers based on rare earth doped bulk materials and fibres. Up-conversion for Sm^{3+} has not yet been reported. Up-conversion can occur through different processes (Fig. 1) [11–13]. One of the most efficient processes leading to up-conversion is the excited state absorption (ESA) which is now reported to occur in Sm^{3+}-doped GdOCl. Initially an ESA process involving a Sm^{3+} impurity was suggested as a reason for a very complex Raman spectra of $M_3Eu(PO_4)_2$ (M=K and Rb) [14].

In this work the Raman spectrum of polycrystalline GdOCl doped with 1 mol% Sm^{3+} was measured at room

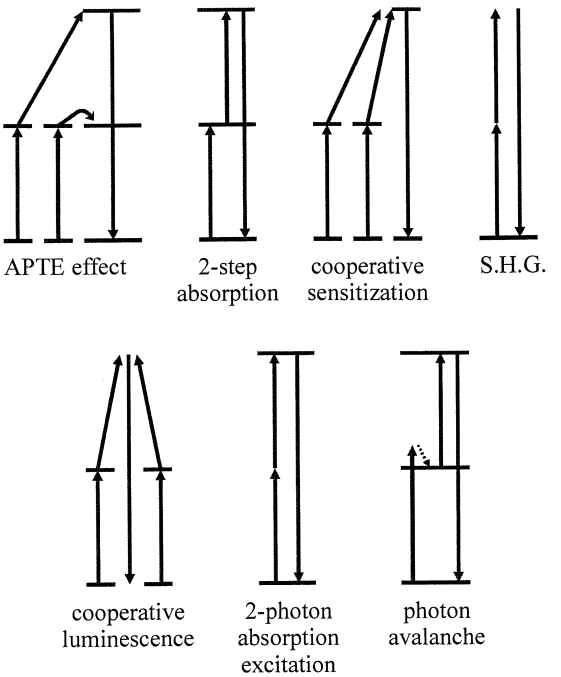

Fig. 1. Up-conversion processes in the RE^{3+} ions [11–13].

☆Presented at the 3rd International Winter Workshop on Spectroscopy and Structure of Rare Earth Systems, Szklarska Poręba/Wroclaw, Poland, April 27–May 1, 1999.

*Corresponding author. Fax: +358-2-333-6730.
E-mail address: jholsa@utu.fi (J. Hölsä)

0925-8388/00/$ – see front matter
PII: S0925-8388(99)00773-2

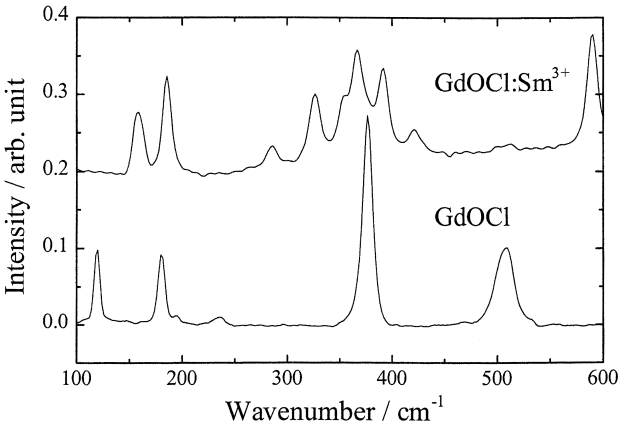

Fig. 2. Comparison of the room temperature Raman spectra of GdOCl and GdOCl:Sm^{3+} ($x_{Sm}=0.01$) using a cw Nd:YAG laser with the wavelength of 1064 nm (9400 cm^{-1}).

Table 1
Free ion and crystal field B_q^k parameters (cm^{-1}) for SmOCl (no. of levels 153; $\sigma=23$ cm^{-1})

Parameter	Value	Parameter	Value	Parameter	Value
F^2	78 167	β	−590	B_0^4	−527
F^4	55 878	γ	1654	B_4^4	±766
F^6	39 779	ζ	1150	B_0^6	1006
α	19.56	B_0^2	−871	B_4^6	±346

temperature using a cw Nd:YAG laser with the excitation wavelength of 1064 nm (9400 cm^{-1}). The resulting spectrum was compared to that of pure GdOCl. The UV–Vis–NIR absorption spectra of GdOCl:Sm^{3+} ($x_{Sm}=0.06$) was measured and the results were compared to the calculated energy levels of Sm^{3+} in SmOCl [15]. The Stokes and anti-Stokes Raman lines of GdOCl:Sm^{3+} ($x_{Sm}=0.01$) were analyzed and compared to the possible luminescence transitions of Sm^{3+}.

2. Experimental

2.1. Sample preparation

The powder samples of SmOCl, GdOCl, and GdOCl:Sm^{3+} ($x_{Sm}=0.01$ and 0.06) were prepared by a solid state reaction between high purity RE_2O_3 and NH_4Cl. In order to avoid any remaining RE_2O_3 a NH_4Cl/RE_2O_3 ratio equal to 2.1 was used. The well homogenized mixtures were heated first at 450°C for 0.5 h followed by recrystallization at 900°C for 1 h in a static N_2 atmosphere. The nitrogen atmosphere was used to prevent the reverse reaction from the oxychloride to oxide. The structure and purity of the products were confirmed by the routine X-ray powder diffraction techniques and no impurity phases were observed.

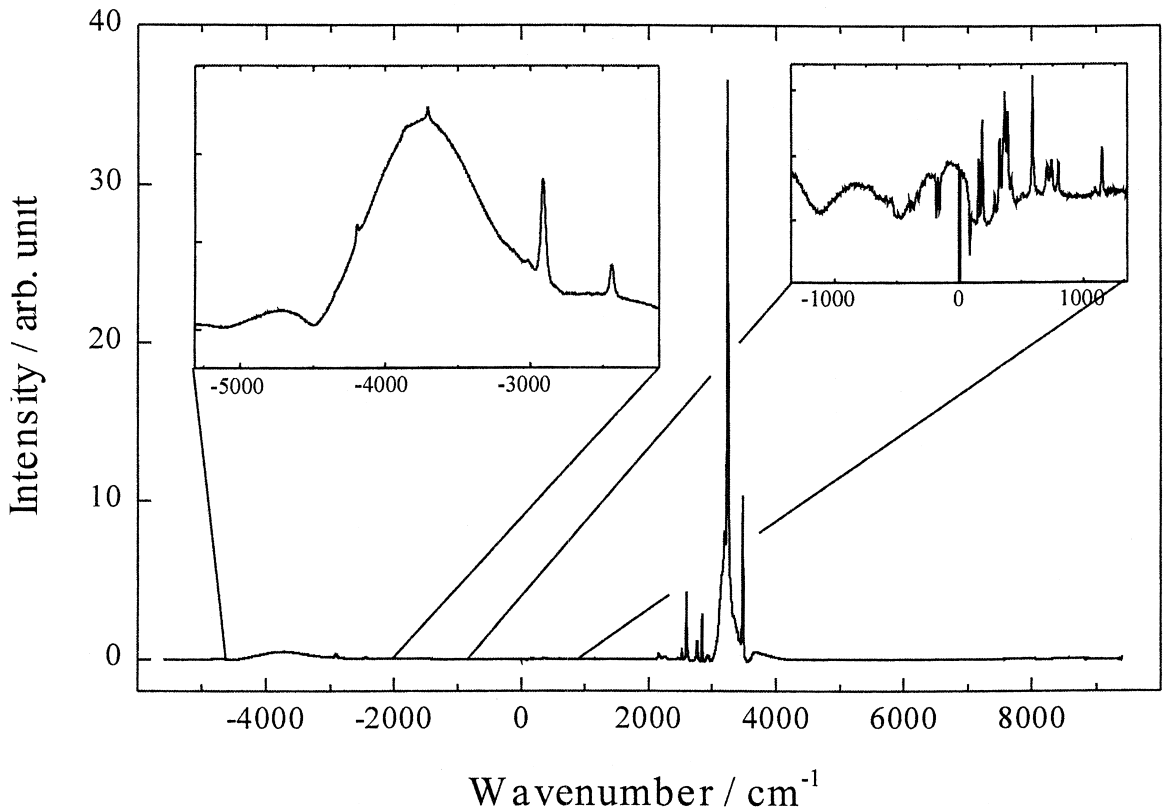

Fig. 3. Room temperature Raman spectrum of GdOCl:Sm^{3+} ($x_{Sm}=0.01$).

Table 2
Experimental and calculated energy levels (cm^{-1}) of SmOCl up to 19 000 cm^{-1}

	$^{2S+1}L_J$ level	E_{obs}	E_{calc}
1	$^6H_{5/2}$		−33
2			248
3			300
Average			172
4	$^6H_{7/2}$		1060
5			1152
6			1278
7			1401
Average			1223
8	$^6H_{9/2}$		2269
9			2310
10			2485
11			2485
12			2591
Average			2428
13	$^6H_{11/2}$		3565
14			3614
15			3786
16			3825
17		3831	3836
18		3902	3907
Average			3756
19	$^6H_{13/2}$	4895	4900
20			5040
21		5152	5164
22		5234	5245
23		5253	5255
24			5275
25			5275
Average			5165
26	$^6H_{15/2}$	6188	6219
27	$^6F_{1/2}$	6410	6462
28	$^6H_{15/2}$	6568	6588
29			6613
30		6631	6630
31			6660
32		6676	6667
33	$^6F_{3/2}$		6703
34			6714
Average			6709
35	$^6H_{15/2}$	6818	6824
36			6872
Average			6634
37	$^6F_{5/2}$	7162	7186
38		7209	7227
39			7264
Average			7226
40	$^6F_{7/2}$	8003	8002
41		8048	8056
42		8069	8083
43		8085	8103
Average		8051	8061
44	$^6F_{9/2}$	9155	9155
45			9189
46		9216	9207
47		9244	9248
48		9270	9271
Average			9214
49	$^6F_{11/2}$		10 507
50		10 522	10 515
51		10 572	10 585
52			10 606
53			10 644
54			10 653
Average			10 585
55	$^4G_{5/2}$	17 703	17 760
56		17 955	18 015
57			18 138
Average			17 971
58	$^4F_{3/2}$	18 889	18 888
59		18 909	18 894
Average		18 899	18 891

2.2. FT-Raman measurements

The room temperature Stokes and anti-Stokes Raman spectra of the polycrystalline GdOCl and GdOCl:Sm^{3+} (x_{Sm}=0.01) were measured with a Bruker FRA 106 FT-Raman accessory. A cw Nd:YAG laser was used at the wavelength of 1064 nm (9400 cm^{-1}). The resolution of the set-up was 4 cm^{-1}.

2.3. Absorption measurements

The UV–Vis–NIR absorption spectra of GdOCl:Sm^{3+} (x_{Sm}=0.06) and SmOCl were obtained with a Varian CARY 5E apparatus in the 200–2700 nm range at 9 K. The instrument reproducibility was better than 2 Å and the band width used was 0.6 Å. The samples were prepared by mixing REOCl with KBr and pressing a transparent disc.

3. Results and discussion

The lighter RE oxychlorides, REOCl, RE=La–Ho, (Er, Y), have the tetragonal PbFCl-type structure [16] with space group $P4/nmm$ ($N°$ 129; Z=2 [17]). The RE and halide atoms reside in a crystallographic 2c site of C_{4v} point symmetry and the oxygen in a 2a site of D_{2d} symmetry [17]. A total of 15 vibrational modes (with acoustical modes excluded) are distributed in the factor group D_{4h} in the following manner [18]:

$$\Gamma_{vib} = 2A_{1g} + 3E_g + B_{2g}(\text{or } B_{1g}) + 2A_{2u} + 2E_u$$

where the gerade (g) vibrations are Raman active and the ungerade (u) vibrations are IR active.

The room temperature Raman spectrum of GdOCl shows five of the six possible lines corresponding to the modes with the irreducible representations $2A_{1g} + 3E_g + B_{1g}$ but the Raman spectrum of GdOCl:Sm^{3+} ($x_{Sm} = 0.01$) is unexpectedly complex (Fig. 2). In addition to the weak Stokes and anti-Stokes Raman lines very strong lines were observed (Fig. 3) in the Stokes region at 2000–4000 cm^{-1}, which is well beyond the conventional Raman lines (~500 cm^{-1}). Also weak lines were observed in the anti-Stokes region from −4500 to −2000 cm^{-1}. Due to the intensity difference of the additional lines between the Stokes and anti-Stokes regions it was suggested that the extra lines result from the Stokes and anti-Stokes luminescence processes. According to expectations the anti-Stokes luminescence is not as efficient as the Stokes luminescence.

The extra lines were subsequently explained by the luminescence processes of Sm^{3+} with the aid of the UV–Vis–NIR absorption spectra of GdOCl:Sm^{3+} ($x_{Sm} = 0.06$) and the energy level simulation (Table 1) of Sm^{3+} in SmOCl [15]. The broad bands observed probably result from the CTS-luminescence of impurity Sm^{2+} impurity which is present due to the weakly reducing atmosphere (NH_3) in the preparation of GdOCl:Sm^{3+}. In the conventional anti-Stokes Raman region a reabsorption process is observed, which causes the sharp line absorption in broad band luminescence.

3.1. Stokes luminescence

Absorption of the Nd:YAG radiation at 9400 cm^{-1} first resulted in the excitation of Sm^{3+} to the $^6F_{9/2}$ level (the crystal field (cf) components are at 9155, 9216, 9244, and 9270 cm^{-1}) (Table 2). The difference is made up with the absorption by the lattice phonons and broadening of the lines at room temperature. Through non-radiative processes the excitation energy migrates to the $^6F_{5/2}$, $^6F_{7/2}$, and $^6H_{15/2}$ levels. Luminescence from the $^6F_{5/2}$ level to the $^6H_{15/2}$ level and from the $^6H_{15/2}$ and $^6F_{7/2}$ levels to the $^6H_{5/2}$ ground level was observed in the Stokes Raman spectrum (Figs. 4a and 5, and Table 3). Transitions between individual Stark level could not be identified because of high temperature leading to population of higher Stark levels of the emitting $^{2S+1}L_J$ levels. Average energies correspond well to the observed lines, however.

3.2. Anti-Stokes luminescence

The excited $^4F_{9/2}$ level of Sm^{3+} absorbs a second Nd:YAG photon at 9400 cm^{-1} and results in the excitation to the $^4F_{3/2}$ level (the cf components are at 18 889 and 18 909 cm^{-1}). The difference is made up with the absorption by the lattice phonons and broadening of the lines at room temperature as before. Luminescence from the $^4F_{3/2}$

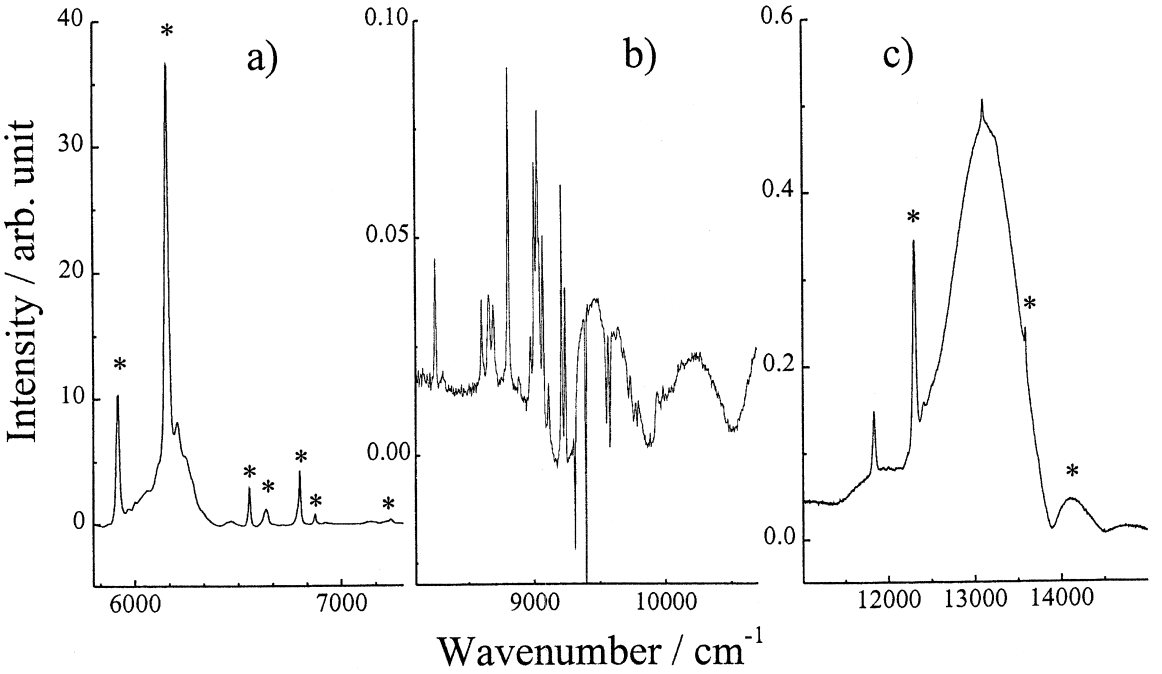

Fig. 4. Parts 5800–7300 (a), 8100–10 700 (b), and 11 000–15 000 cm^{-1} (c) of the Stokes and anti-Stokes Raman spectrum of GdOCl:Sm^{3+} ($x_{Sm} = 0.01$) at room temperature converted to absolute energies. The lines concluded to result from the luminescence of Sm^{3+} are marked with an asterisk.

Table 3
Lines in the Raman spectrum resulting from the luminescence processes of Sm^{3+} in GdOCl

Transition	Calculated energy range (cm^{-1})[a]	Experimental (cm^{-1})
Stokes luminescence		
$^6H_{15/2} \rightarrow {}^6H_{5/2}$	5888–6818	5921, 6156 6555, 6800
$^6F_{7/2} \rightarrow {}^6H_{7/2}$	6602–7025	6634
$^6F_{5/2} \rightarrow {}^6H_{5/2}$	6862–7209	6875, 7139, 7242
Anti-Stokes luminescence		
$^4F_{3/2} \rightarrow {}^6H_{15/2}$	12 071–12 721	12 310
$^4F_{3/2} \rightarrow {}^6H_{13/2}$	13 636–13 994	13 596
$^4G_{5/2} \rightarrow {}^6H_{11/2}$	13 801–14 390	14 126

[a] Calculated from the crystal field splitting of the corresponding excited and ground state.

level to the $^6H_{15/2}$ and $^6H_{13/2}$ levels was observed in the anti-Stokes Raman spectrum (Figs. 4c and 5, and Table 3). Through non-radiative processes the energy migrated from the $^4F_{3/2}$ level to the $^4G_{5/2}$ level from which luminescence to the $^6H_{11/2}$ level was observed in the anti-Stokes spectrum (Figs. 4c and 5, and Table 3). Unfortunately, luminescence from the $^4F_{3/2}$ and $^4G_{5/2}$ levels to levels lower than $^6H_{11/2}$ were not observed due to the limited spectral range of the FT-Raman accessory used.

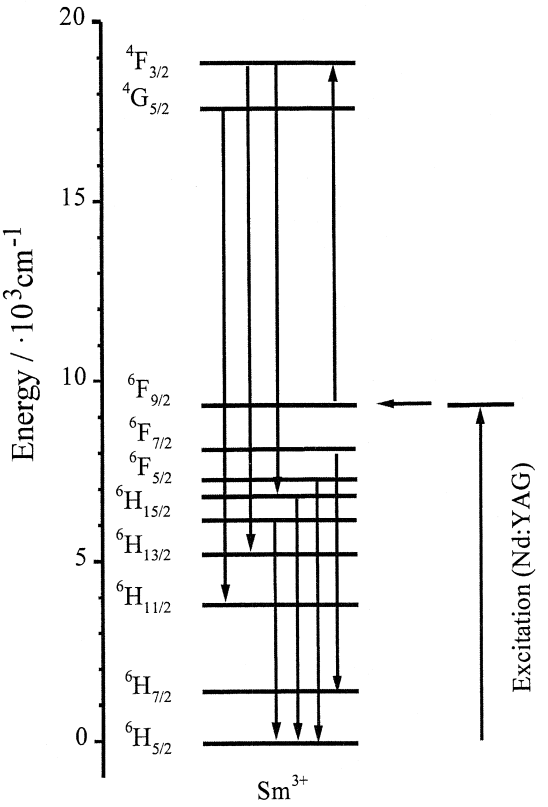

Fig. 5. Simplified energy level diagram of the Sm^{3+} ion showing the ESA and possible luminescence processes observed in the Raman spectrum of GdOCl:Sm^{3+} ($x_{Sm}=0.01$).

4. Conclusions

ESA and up-conversion luminescence of Sm^{3+} in GdOCl was observed in the Raman spectrum of GdOCl:Sm^{3+} ($x_{Sm}=0.01$). Most of the unconventional Raman lines were proved to result from Stokes and anti-Stokes luminescence of Sm^{3+}. However, a few lines were not explained and the broad bands require further considerations. Further studies include luminescence measurements at different temperatures and with different doping levels of Sm^{3+}. Also dynamic luminescence measurements will be carried out at different experimental conditions and the effect of the host lattice will be investigated.

Acknowledgements

Financial support from the Academy of Finland and the Graduate School of Materials Research (Turku, Finland) is acknowledged. Some of the rare earth oxides used were provided by Rhodia SA.

References

[1] L.F. Johnson, H.J. Guggenheim, Appl. Phys. Lett. 19 (1971) 44.
[2] F. Auzel, Proc. IEEE 61 (1973) 758.
[3] J.C. Wright, Topics Appl. Phys. 15 (1976) 239.
[4] W. Lenth, R.M. Macfarlane, J. Lumin. 45 (1990) 346.
[5] W. Lenth, R.M. Macfarlane, Opt. Photon News 3 (1992) 8.
[6] R.G. Smart, D.C. Hanna, A.C. Tropper, S.T. Davey, S.F. Carter, D. Szebesta, Electron. Lett. 27 (1991) 1307.
[7] R.A. Macfarlane, Appl. Phys. Lett. 54 (1989) 2301.
[8] F. Tong, W.P. Risk, R.M. Macfarlane, W. Lenth, Electron. Lett. 25 (1989) 1389.
[9] P. Xie, S.C. Rand, Opt. Lett. 15 (1990) 848.
[10] J.P. Jouart, M. Bouffard, G. Klein, G. Mary, J. Lumin. 60–61 (1994) 93.
[11] F. Auzel, in: B. Jezowska-Trzebiatowska, J. Lengendziewicz, W. Stręk (Eds.), Rare Earth Spectroscopy, World Scientific, Singapore, 1994, p. 502.

[12] G. Blasse, B.C. Grabmaier (Eds.), Luminescent Materials, Springer, Berlin, 1994, p. 196.
[13] M.-F. Joubert, in: Third Int. Winter Workshop on Spectroscopy and Structure of Rare Earth Systems, Szklarska Poreba, Poland, April 27–May 1, 1999, p. O11.
[14] M. Kloss, J. Hölsä, H. Rahiala, L. Schwarz, D. Haberland, in: Jabloński Cent. Conf. Lumin. Photophys., Torun, Poland, July 23–27, 1998, p. 77.
[15] J. Hölsä, J. Korventausta, R.-J. Lamminmäki, E. Säilynoja, P. Porcher, J. Lumin. 72–74 (1997) 204.
[16] L.H. Brixner, E.P. Moore, Acta Crystallogr., Sect. C 39 (1983) 1316.
[17] N.F.M. Henry, K. Lonsdale (Eds.), International Tables of Crystallography, Vol. 1, Kynoch Press, Birmingham, 1969.
[18] Y. Hase, L. Dunstan, M.L.A. Temperini, Spectrochim. Acta A 37 (1981) 597.